Phys. Status Solidi B **253,** No. 10, 2079–2084 (2016) / **DOI** 10.1002/pssb.201600363

physica status solidi b
www.pss-b.com
basic solid state physics

Reassessment of the recombination properties of aluminium–oxygen complexes in n- and p-type Czochralski-grown silicon

Chang Sun*[,1], Fiacre E. Rougieux[1], Julien Degoulange[2], Roland Einhaus[2], and Daniel Macdonald[1]

[1] Research School of Engineering, The Australian National University, Canberra, ACT 2601, Australia
[2] Apollon Solar, 66 Cours Charlemagne, Lyon 69002, France

Received 27 June 2016, revised 17 July 2016, accepted 6 August 2016
Published online 23 August 2016

Keywords aluminium, charge carrier lifetimes, charge carrier recombination, defect complexes, lifetime spectroscopy, oxygen, silicon

* Corresponding author: e-mail chang.sun@anu.edu.au, Phone: +61 2 612 555 38, Fax: +61 2 6125 0506

The recombination parameters of aluminium–oxygen complexes in silicon have been reassessed by applying lifetime spectroscopy on several n- and p-type intentionally Al-contaminated and control samples, using a single-level defect model. The presence of the control samples has allowed greater accuracy for the extraction of the recombination lifetime. The uncertainty ranges of the parameters have been tightened significantly by simultaneously fitting the lifetime on several samples. The electron/hole capture cross section ratio k was reassessed to be 380, in the uncertainty range of 330–460. A direct comparison of the n- and p-type samples has shown that those complexes are much more recombination-active in p-type silicon than in n-type silicon at low and intermediate injection levels.

1 Introduction Aluminium is a common metallic impurity in solar-grade silicon materials. Concentrations in the range of 10^{14}–10^{17} cm^{-3} are typical in the upgraded metallurgical silicon (UMG-Si) wafers after ingot growth [1]. Al is more difficult to remove through directional solidification than many transition metals, considering that the segregation coefficient of Al is $k_{Al} = 2 \times 10^{-3}$ [2–4], in comparison with Fe with $k_{Fe} = 6.4 \times 10^{-6}$ [5], Ni with $k_{Ni} = 3.2 \times 10^{-5}$ [5, 6], and Cu with $k_{Cu} = 8 \times 10^{-4}$ [5, 7]. Also, because of its low diffusivity [8], it is not efficient to remove Al through gettering once present in the wafers. The detrimental effects of Al on the carrier lifetime of Czochralski-grown (Cz) silicon wafers are widely recognised, and numerous authors have attributed the effects to the recombination-active aluminum–oxygen (Al–O) complexes [4, 5, 9–15].

Previous studies on the recombination properties of Al–O complexes have been based on deep-level transient spectroscopy (DLTS) [4, 5, 9, 12] or temperature- and/or injection-dependent lifetime spectroscopy (TIDLS or IDLS) [11, 12]. With DLTS, the energy level can be accurately determined, but generally only the majority-carrier capture cross section is accessible [16]. In contrast, the lifetime spectroscopy methods are based on the Shockley-Read-Hall (SRH) model [17, 18], and can be used to determine the electron/hole capture cross section ratio k [11, 19]. However, they have a large uncertainty range for the energy level of deep levels, and it is generally not possible to separate the capture cross section from the defect concentration if both are unknown, as this technique only determines their product [11, 19]. Table 1 lists the recombination parameters of Al–O complexes from the literature. The deep level located at 0.38–0.50 eV above the valence band E_v, having a most probable value around 0.44 eV, is consistent among the different studies applying DLTS [4, 5, 9, 12]. However, k varies across orders of magnitudes in the literature. Both of the previous lifetime spectroscopy studies assumed a second shallow level to obtain a reasonable fit over the entire injection range [11, 12]. However, the shallow level has not been detected by any DLTS studies, and thus remains unconfirmed. In addition, in the absence of control samples, the authors assumed the effective lifetime to be the bulk SRH recombination lifetime [11], or obtained the SRH lifetime

Table 1 Recombination parameters of the Al–O complex from the literature and found in this work.

authors	E_t–E_v (eV)	σ_n (cm^2)	σ_p (cm^2)	k	methods	refs.
Marchand et al.	0.397 ± 0.005 0.314 ± 0.002 0.215 ± 0.001		$(8.6 \pm 0.7) \times 10^{-17}$ $(6.6 \pm 0.2) \times 10^{-15}$ $(9.2 \pm 0.5) \times 10^{-22}$		DLTS	[4, 9]
Davis et al.	0.43 ± 0.05 0.47 ± 0.03	1.4×10^{-14}	5.7×10^{-15}	2.5	DLTS	[5]
Schmidt	0.22–0.68 0.14 or 0.98			90	TIDLS	[11]
Rosenits et al.	0.44 ± 0.02 0.15	3.1×10^{-10}	3.6×10^{-13}	870	DLTS and IDLS IDLS	[12]
this work				380 (−50, +80)	IDLS	

by correcting the measured effective lifetime with a modelled intrinsic recombination lifetime [12]. In principle, this can cause uncertainties in the fitted SRH lifetimes, and may also explain why a second shallow level was required in those studies.

In this work, we conduct a new IDLS analysis using a single-level model applied to several n- and p-type Cz wafers that have been intentionally contaminated with Al and control wafers, to reassess the recombination parameters of the defect. The control samples allow the SRH lifetime to be extracted with greater accuracy. Simultaneously, performing IDLS on several samples helps tighten the uncertainty ranges of the parameters [20], while having both n- and p-type of samples enables the recombination activity of the defect in both types of silicon to be directly compared.

2 Experimental The samples investigated in this study were from four B- and P-doped compensated Czochralski (Cz) ingots supplied by Apollon Solar. The ingots were grown from 9N poly silicon feedstock that was intentionally doped with boron and phosphorus to simulate compensated UMG-Si [21]. For each type, one was grown as a control ingot and the other was intentionally contaminated with Al. The concentration of boron in the starting melt was 1.32×10^{16} cm^{-3} in all four ingots. The concentration of Al ([Al]) in the starting melt was 1.04×10^{17} cm^{-3} in the Al-doped ingots. The concentration of phosphorus in the starting melt of the n- and p-type ingots were 3.64×10^{16} cm^{-3} and 7.73×10^{15} cm^{-3}, respectively. The ingots were cut to wafers, and three p-type and one n-type Al-contaminated wafers and the corresponding control wafers were chosen for this study. Some key parameters of the samples are listed in Table 2. The net doping levels and the [Al] were calculated applying the Scheil's law [22]. The segregation coefficients of B, P and Al were taken as 0.8, 0.35 and 0.002, respectively [2–4]. The resistivities were measured by dark conductance, and were also predicted applying Schindler et al.'s mobility model for compensated silicon, based on the expected dopant concentrations using the Scheil's law [23]. The predicted values mostly lie within 10% of the measured values, as shown in the table. The interstitial oxygen concentrations ([O_i]) in the central region of the samples were determined by the OXYMAP technique [24].

The samples were chemically etched to remove saw damage, and then went through a phosphorus gettering process at 880 °C for 0.5 h, and 600 °C for about 14 h [25]. Performing the extended heat treatment at a lower temperature (600 °C for 14 h) after the diffusion was found

Table 2 Parameters of the samples in this study. Note that g represents the solidified fraction.

samples	modelled net doping (cm^{-3})	modelled [Al] (cm^{-3})	ρ measured with QSSPC ($\Omega \cdot$ cm)	ρ predicted by Schindler et al.'s mobility model ($\Omega \cdot$ cm)	[O_i] (cm^{-3})
p-type control ($g = 0.03$)	7.9×10^{15}	0	1.96	2.06	1.3×10^{18}
p-type control ($g = 0.23$)	7.9×10^{15}	0	1.94	2.05	1.1×10^{18}
p-type control ($g = 0.43$)	7.9×10^{15}	0	1.99	2.06	9.9×10^{17}
p-type + Al ($g = 0.02$)	8.1×10^{15}	2.1×10^{14}	2.23	2.00	1.2×10^{18}
p-type + Al ($g = 0.20$)	8.2×10^{15}	2.6×10^{14}	2.20	1.98	1.1×10^{18}
p-type + Al ($g = 0.56$)	8.3×10^{15}	4.7×10^{14}	2.25	1.98	8.4×10^{17}
n-type control ($g = 0.65$)	1.2×10^{16}	0	0.49	0.58	8.4×10^{17}
n-type + Al ($g = 0.64$)	1.1×10^{16}	5.8×10^{14}	0.53	0.63	8.1×10^{17}

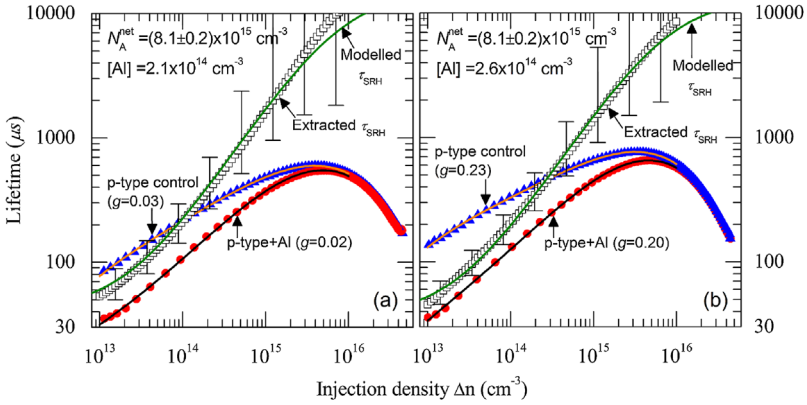

Figure 1 Injection-dependent lifetimes of the samples (a) p-type + Al ($g = 0.02$) and (b) p-type + Al ($g = 0.20$) and the corresponding control samples. The extracted and the modelled SRH recombination lifetimes are also shown.

to increase the efficiency in removing fast diffusing metallic impurities [25]. Those impurities were present in all the samples before gettering, resulting in a reduced difference in the lifetimes of the control samples and the Al-contaminated samples. As confirmed by dark conductance and Fourier Transform Infrared (FT-IR) spectrophotometry measurements, the resistivity and [O_i] remained unchanged, within measurement uncertainty, before and after the gettering step. After gettering, another 10 μm was etched from both sides, followed by surface passivation with plasma-enhanced chemical vapour deposited (PECVD) SiN_x films. The injection-dependent lifetimes were measured with the quasi-steady-state photoluminescence (QSSPL) method, to avoid trapping effects at low injection levels [26]. The samples were annealed at 260 °C for 30 min in the dark to deactivate the boron–oxygen (BO) complexes before the measurements.

3 Modelling procedure To extract the SRH recombination lifetimes τ_{SRH} due to Al–O complexes, we determined polynomial fits for the measured lifetimes of the Al-contaminated and control samples, and then calculated τ_{SRH} applying $1/\tau_{SRH} = 1/\tau_{eff} - 1/\tau_{control}$. The polynomial curves allowed convenient interpolation between the two sets of data points. Only lifetime data at injection levels lower than $\Delta n = 1 \times 10^{16}\,cm^{-3}$ were used to extract τ_{SRH}. At injection levels higher than this, the lifetimes of the control sample and the Al-contaminated sample are almost identical (shown in Section 4). This causes large uncertainties in the extracted τ_{SRH}, adversely affecting the subsequent fitting of the recombination parameters.

The extracted τ_{SRH} of the three p-type Al-contaminated samples were then fitted simultaneously to determine k. As will be discussed in Section 4, there is no significant difference in lifetime between the two n-type samples, which would result in large uncertainties in the extracted $\tau_{SRH,n\text{-}type}$. So the n-type samples were not included in the fitting but were subsequently used to check for consistency with the parameters extracted from the p-type samples.

The extraction of the SRH lifetime using a control sample has the advantage of removing the effect of surface recombination velocity and intrinsic recombination on the extracted SRH lifetime. Contrary to previous studies using no control samples [11, 12], we found that a single deep level model could describe the p-type SRH lifetimes very well, and the n-type lifetime across most of the injection level range (the shallow defect affecting the high injection part of the lifetime in previous study was most likely related to intrinsic recombination or surface recombination but not bulk SRH recombination). Hence only the deep

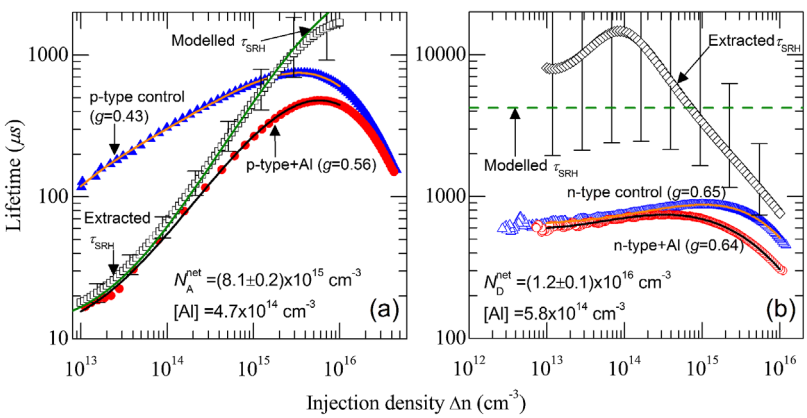

Figure 2 Injection-dependent lifetimes of the samples (a) p-type + Al ($g = 0.56$) and (b) n-type + Al ($g = 0.64$) and the corresponding control samples. The extracted and the modelled SRH recombination lifetimes are also shown. Note that the vertical axes of the two figures are not in the same scale.

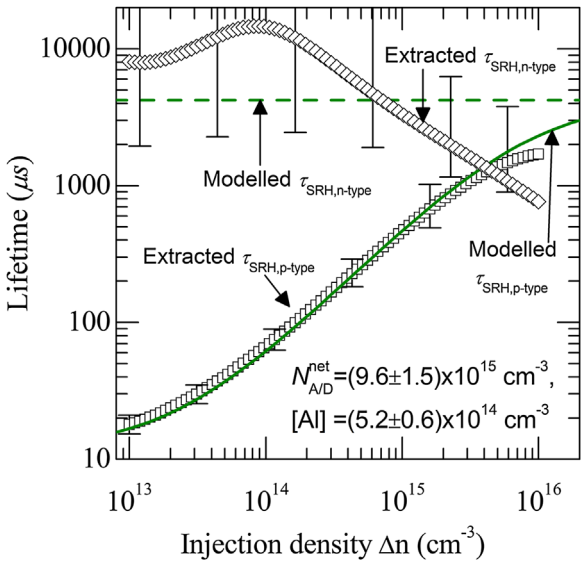

Figure 3 The extracted and modelled SRH lifetime of the Al–O complexes in the samples n-type + Al ($g = 0.64$) and p-type + Al ($g = 0.56$).

level $E_t = E_v + (0.38\text{–}0.50)$eV was considered in the model [4, 5, 9, 12]. When E_t lies in this range, both p_1 and kn_1 are negligible compared with the doping unless $k > 1000$, which is not true in this case as confirmed by the fitting. Thus the uncertainties in the energy level will not impact on the fitting of k. For the same reason, it was impossible to obtain the energy level via IDLS in this work. The absolute values of the capture cross sections could not be extracted either, due to the unknown concentrations of the defect complexes. Normally when fitting the lifetime, $\sum(\tau_{\text{fitted}} - \tau_{\text{measured}})^2$ is minimized. However, when the lifetime crosses several orders of magnitudes, this method unintentionally allocates larger weights to the higher-value lifetime data. To avoid this problem, $\sum[(\tau_{\text{fitted}} - \tau_{\text{measured}})/\tau_{\text{measured}}]^2$ was minimized in the fitting to determine the optimal k in this work. The uncertainty range of k was determined as follows: for every k value varied in the range of 0–10 000, with the extracted lifetime data, an optimal value of $N_t\sigma_n$ can be determined for each sample, where N_t is the defect concentration in the corresponding sample, and σ_n is the electron capture cross section. With the determined $N_t\sigma_n$ and the k value, we can model the lifetime data for each sample. Then the modelled lifetime τ_{fitted} is compared with the extracted lifetime τ_{measured}. A feasible k is selected if τ_{fitted} totally lies within the error bars of τ_{measured} for every sample. The uncertain range of k is the set of all the selected feasible values.

4 Results and discussion Figure 1 shows the lifetime measurements for the samples p-type + Al ($g = 0.02$) and p-type + Al ($g = 0.20$) and the corresponding control samples. The third group of p-type samples, p-type + Al ($g = 0.56$) and its control sample are shown in Fig. 2(a). The polynomial fits are shown in solid lines in Figs. 1 and 2, agreeing very well with the measured data. The extracted SRH recombination lifetimes τ_{SRH} are also shown in the figures. The error bars were calculated assuming 12% error in the measured lifetimes [27]. As shown in the figures, the extracted τ_{SRH} is strongly injection-dependent in p-type silicon (p-Si), increasing by two orders of magnitudes from $\Delta n = 1 \times 10^{13}\,\text{cm}^{-3}$ to $\Delta n = 1 \times 10^{16}\,\text{cm}^{-3}$.

The lifetime measurements of the n-type samples and the extracted τ_{SRH} are shown in Fig. 2(b). Throughout the measured injection range, there is very little difference in lifetime between the two samples, indicating that Al–O complexes are weakly recombination-active in n-type silicon (n-Si). The humped shape of the extracted τ_{SRH} can be attributed to the uncertainties, as shown by the large error bars. The n- and p-type Al-contaminated samples shown in Fig. 2 have similar net doping levels, [Al] and [O_i], thus it is reasonable to assume similar concentrations of Al–O complexes in both samples. Figure 3 directly compares the extracted τ_{SRH} in the two samples. By comparison, this defect is more recombination-active in p-Si than n-Si at low and intermediate injection levels. At high-injection level, the two lifetime curves lie within each other's error bars.

Figure 4 shows $\sum[(\tau_{\text{fitted}} - \tau_{\text{measured}})/\tau_{\text{measured}}]^2$ as a function of k. The optimal value of k was determined to be 380, in the uncertainty range of 330–460. As shown by Table 1, this value lies between the other values in the literature. The optimal value was then used to model the $\tau_{\text{SRH,p-type}}$ for the p-type samples, which agreed well with the extracted data from the experiments (Figs. 1–3).

The value of $N_t\sigma_n$ could be derived for each p-type Al-contaminated sample. Assuming the same defect concentration in the samples p-type + Al ($g = 0.56$) and n-type + Al ($g = 0.64$), τ_{SRH} could be modelled for the

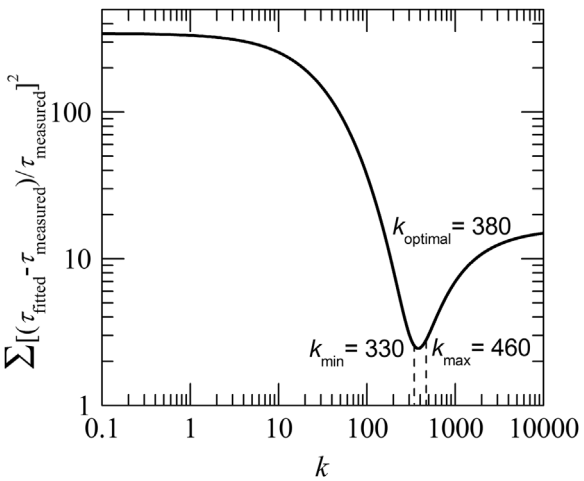

Figure 4 $\sum[(\tau_{\text{fitted}} - \tau_{\text{measured}})/\tau_{\text{measured}}]^2$ as a function of k, when simultaneously fitting the three extracted $\tau_{\text{SRH,p-type}}$.

n-type sample. As shown in Fig. 2(b), the modelled $\tau_{SRH,n\text{-}type}$ lies mostly within the error bars of the extracted $\tau_{SRH,n\text{-}type}$ from the measurements, indicating that the same deep level can explain the measured lifetimes for the n-type samples, except possibly at the highest injection levels. The modelled $\tau_{SRH,n\text{-}type}$ is injection-independent, because when both n_1 and p_1 are negligible, and $k \gg 1$, the lifetime is $\tau_{SRH,n\text{-}type} = k/N_t\sigma_n v_{th}$. Note that this is also the expression for the high-injection lifetime regardless of the doping when $k \gg 1$. As shown in Fig. 3, the modelled $\tau_{SRH,p\text{-}type}$ coincides with the modelled $\tau_{SRH,n\text{-}type}$ at high injection levels. $\tau_{SRH,n\text{-}type}$ is injection-independent so the complexes are not very recombination-active over the entire injection range in n-Si. While at low injection levels in p-Si, $\tau_{SRH,p\text{-}type,low\text{-}injection} = 1/N_t\sigma_n v_{th}$, degrading by the factor k. As directly compared in Fig. 3, at low and intermediate injection levels, which are more relevant to standard solar cell operating conditions, both the experimental data and the modelling results show that the Al–O complexes are much more recombination-active in p-Si than n-Si.

5 Conclusions The recombination parameters of Al–O complexes in silicon have been reassessed by applying IDLS, using n- and p-type Cz silicon wafers that have been intentionally contaminated with Al and control wafers, and assuming only a single, deep defect level. The single deep level explains the measured lifetimes in p-Si very well, and in n-Si across most of the injection level range of interest. The electron/hole capture cross section ratio k was reassessed to be 380 (-50, $+80$). Both experimental and modelling results show that Al–O complexes have much greater impact on the carrier lifetimes in p-Si than n-Si at low and intermediate injection levels. Concerning the potential impact of Al contamination on cell performance in low-cost solar-grade materials, n-Si is potentially a better choice.

Acknowledgements This work has been supported through the Australian Renewable Energy Agency (ARENA) project RND009 and the Australian Centre for Advanced Photovoltaics. Support from the Australian Research Council (ARC) DECRA and Future Fellowships programs are also acknowledged. The authors would like to thank Nicolas Enjalbert of CEA-INES for the OXYMAP measurements.

References

[1] S. Pizzini, Advanced Silicon Materials for Photovoltaic Applications (Wiley, Hoboken, NJ, 2012).
[2] H. Kodera, Diffusion coefficients of impurities in silicon melt, Jpn. J. Appl. Phys. **2**, 212–219 (1963).
[3] B. Bathey and M. Cretella, Solar-grade silicon, J. Mater. Sci. **17**, 3077–3096 (1982).
[4] R. L. Marchand and C. T. Sah, Study of thermally induced deep levels in Al doped Si, J. Appl. Phys. **48**, 336–341 (1977).
[5] J. R. Davis Jr, A. Rohatgi, R. Hopkins, P. Blais, P. Rai-Choudhury, J. McCormick, and H. Mollenkopf, Impurities in silicon solar cells, IEEE Trans. Electron Devices **27**, 677–687 (1980).
[6] R. Hopkins, R. Seidensticker, J. Davis, P. Rai-Choudhury, P. Blais, and J. McCormick, Crystal growth considerations in the use of "solar grade" silicon, J. Cryst. Growth **42**, 493–498 (1977).
[7] R. Hopkins and A. Rohatgi, Impurity effects in silicon for high efficiency solar cells, J. Cryst. Growth **75**, 67–79 (1986).
[8] O. Krause, H. Ryssel, and P. Pichler, Determination of aluminum diffusion parameters in silicon, J. Appl. Phys. **91**, 5645–5649 (2002).
[9] R. L. Marchand, A. R. Stivers, and C. Sah, Recombination centers in aluminum-doped silicon diffused in high phosphorus concentration, J. Appl. Phys. **48**, 2576–2580 (1977).
[10] F. Shimura, T. Okui, and T. Kusama, Noncontact minority-carrier lifetime measurement at elevated temperatures for metal-doped Czochralski silicon crystals, J. Appl. Phys. **67**, 7168–7171 (1990).
[11] J. Schmidt, Temperature- and injection-dependent lifetime spectroscopy for the characterization of defect centers in semiconductors, Appl. Phys. Lett. **82**, 2178–2180 (2003).
[12] P. Rosenits, T. Roth, S. W. Glunz, and S. Beljakowa, Determining the defect parameters of the deep aluminum-related defect center in silicon, Appl. Phys. Lett. **91**, 122109 (2007).
[13] J. Schmidt, N. Thiemann, R. Bock, and R. Brendel, Recombination lifetimes in highly aluminum-doped silicon, J. Appl. Phys. **106**, 93707 (2009).
[14] R. Bock, P. P. Altermatt, J. Schmidt, and R. Brendel, Formation of aluminum-oxygen complexes in highly aluminum-doped silicon, Semicond. Sci. Technol. **25**, 105007 (2010).
[15] T. Shi, W.-J. Yin, Y. Wu, M. Al-Jassim, and Y. Yan, The structure and properties of (aluminum, oxygen) defect complexes in silicon, J. Appl. Phys. **114**, 063520 (2013).
[16] K. Graff, Metal Impurities in Silicon-Device Fabrication (Springer, Berlin, Heidelberg, New York, 2000).
[17] W. Shockley and W. Read Jr, Statistics of the recombinations of holes and electrons, Phys. Rev. **87**, 835 (1952).
[18] R. N. Hall, Electron-hole recombination in germanium, Phys. Rev. **87**, 387 (1952).
[19] S. Rein, Lifetime Spectroscopy: A Method of Defect Characterization in Silicon for Photovoltaic Applications (Springer, Berlin, Heidelberg, New York, 2006).
[20] C. Sun, F. E. Rougieux, and D. Macdonald, Reassessment of the recombination parameters of chromium in n-and p-type crystalline silicon and chromium-boron pairs in p-type crystalline silicon, J. Appl. Phys. **115**, 214907 (2014).
[21] J. Degoulange, N. Enjalbert, S. Dubois, R. Einhaus, F. Cocco, D. Grosset-Bourbange, P. Rivat, and Y. Delannoy, Evaluation of the electrical properties of intentionally Al and Fe contaminated p-type Cz Si ingots: from feedstock to solar cells, in: Proceedings of the 30th European Photovoltaic Solar Energy Conference, 2015, pp. 600–604.
[22] E. Scheil, Prediction of mierosegregation in alloys, Z. Metallkd. **34**, 70 (1942).
[23] F. Schindler, M. C. Schubert, A. Kimmerle, J. Broisch, S. Rein, W. Kwapil, and W. Warta, Modeling majority carrier mobility in compensated crystalline silicon for solar cells, Sol. Energy Mater. Sol. Cells **106**, 31–36 (2012).

[24] J. Veirman, S. Dubois, N. Enjalbert, and M. Lemiti, A fast and easily implemented method for interstitial oxygen concentration mapping through the activation of thermal donors in silicon, Energy Proc. **8**, 41–46 (2011).
[25] J. Härkönen, V. Lempinen, T. Juvonen, and J. Kylmäluoma, Recovery of minority carrier lifetime in low-cost multicrystalline silicon, Sol. Energy Mater. Sol. Cells **73**, 125–130 (2002).
[26] T. Trupke and R. Bardos, Photoluminescence: a surprisingly sensitive lifetime technique, in: 31st IEEE Photovoltaic Specialists Conference, 2005, pp. 903–906.
[27] Z. Hameiri, K. R. McIntosh, and T. Trupke, Uncertainty in photoluminescence-based effective carrier lifetime measurements, in: 38th IEEE Photovoltaic Specialists Conference, 2012, pp. 390–395.

